

Thermal stability and rehybridization of carbon bonding in tetrahedral amorphous carbon

D. S. Grierson,^{1,a)} A. V. Sumant,² A. R. Konicek,³ T. A. Friedmann,⁴ J. P. Sullivan,⁴ and R. W. Carpick⁵

¹*Department of Mechanical Engineering, University of Wisconsin-Madison, Madison, Wisconsin 53706, USA*

²*Center for Nanoscale Materials, Argonne National Laboratory, Argonne, Illinois 60439, USA*

³*Department of Physics & Astronomy, University of Pennsylvania, Philadelphia, Pennsylvania 19104, USA*

⁴*Sandia National Laboratories, Albuquerque, New Mexico 87185, USA*

⁵*Department of Mechanical Engineering and Applied Mechanics, University of Pennsylvania, Philadelphia, Pennsylvania 19104, USA*

(Received 21 July 2009; accepted 6 December 2009; published online 11 February 2010)

We perform a quantitative investigation of the energetics of thermally induced $sp^3 \rightarrow sp^2$ conversion of carbon-carbon bonds in tetrahedral amorphous carbon (ta-C) films by using near-edge x-ray absorption fine structure (NEXAFS) and Raman spectroscopy. We investigate the evolution of the bonding configuration in ta-C thin films subjected to high temperature annealing in flowing Argon gas using a rapid thermal annealing furnace over the range of 200–1000 °C. We observe no substantial change in bonding structure below 600 °C. Changes in the NEXAFS and Raman spectra start to appear above 600 °C, and by 1000 °C a significant increase in the sp^2 bonding in the film is observed. No oxygen bonding is detected in the NEXAFS spectra, but we do observe an isosbestic point, demonstrating that the thermally driven $sp^3 \rightarrow sp^2$ conversion reaction occurs without passing through an intermediate transition state. This allows us to use NEXAFS spectra of thermally annealed ta-C films to quantitatively determine that the activation energy for directly converting the sp^3 -bonded carbon to the sp^2 -bonded configuration is 3.5 ± 0.9 eV. © 2010 American Institute of Physics. [doi:10.1063/1.3284087]

I. INTRODUCTION

Carbon-based materials exist in a range of forms, such as graphite, diamond, amorphous carbon (a-C), nanotubes, fullerenes (C_{60}), graphene,¹ and diamondoids,² many of which have remarkable properties. The properties of these materials are largely affected by the hybridization state and ordering of the carbon-carbon bonds (i.e., sp , sp^2 , and sp^3). The structural configuration of these bonds, and their energetics and kinetics, have important effects on material properties and thermal stability. Knowing the hybridization state and detecting rehybridization of carbon is important but challenging to realize experimentally in a quantitative fashion. One form of a-C in which the hybridization state of the bonds plays a dominant role in the material's mechanical, electrical, and thermal properties is tetrahedral amorphous carbon (ta-C).

There is significant interest in studying ta-C, a specific type of hydrogen-free, hard, and amorphous carbon film, because it has several unique properties that are close to those of diamond. It has excellent mechanical (hardness: ~ 80 GPa, Young's modulus: 710–805 GPa) (Refs. 3–7) and macroscale tribological (friction coefficient: < 0.1 – 0.25) (Refs. 8–11) properties, and the as-grown surface is hydrophobic and chemically inert. In addition, ta-C films are optically transparent, moderately conductive, and can be atomically smooth (~ 0.1 – 1 nm rms roughness, depending on the

growth substrate and deposition parameters).^{12–18} It can also be processed to have low residual stress, as discussed further below. ta-C is best described as an amorphous mixture of nanophases of tetrahedrally coordinated (sp^3) carbon, comprising about 75–85 at. % of the total, and trigonally coordinated (sp^2) carbon making up the remainder. The trigonally bonded carbon is not randomly distributed but is instead clustered as conjugated chain- or sheetlike structures which are responsible for the electrical conductivity in this material.¹³ This allows for fabrication of structures, such as electrically actuated microelectromechanical systems (MEMSs), out of ta-C without the need for doping.¹⁹

The ta-C studied here is deposited at room temperature using an energetic pure carbon beam that contains a significant fraction of carbon ions with energies peaked near 100 eV. The ablation plume is created by focusing a pulsed excimer laser ($\lambda = 248$ nm) onto a graphite target. Because of subsurface implantation of the energetic carbon species, these films typically exhibit extremely high levels of compressive stress (~ 2 – 8 GPa). Since ta-C is a desirable material for MEMS, post-deposition stress relief is critical. With suitable control of film deposition, 100% stress relief (down to zero ± 10 MPa) can be achieved in these films by either thermal annealing^{5,12} for a period of minutes at a temperature of ~ 650 °C or laser annealing at higher temperatures for nanoseconds.²⁰ High-quality ta-C films can also be deposited using the filtered cathodic arc method.^{14,21}

Other research groups have used various characterization techniques to study the bonding configuration in ta-C upon

^{a)}Author to whom correspondence should be addressed. Electronic mail: dsgrrierson@wisc.edu.

thermal annealing. Ferrari *et al.* were the first to investigate changes in the bonding configuration of ta-C, deposited by the filtered cathodic vacuum arc technique, due to thermal annealing.¹⁴ Using electron energy loss spectroscopy (EELS) and ultraviolet Raman spectroscopy, they observed that the sp^3 fraction (initially at $\sim 87\%$) remains constant up to a temperature of ~ 700 °C, decreases slightly up to 1100 °C, and then drops dramatically to $<20\%$ at 1200 °C. Using visible Raman spectroscopy, they confirmed that a small but resolvable decrease in the sp^3 fraction occurs in films annealed above 800 °C. Alam *et al.*¹² used nuclear magnetic resonance (NMR) spectroscopy to reveal that the sp^3 content of an initially 82% sp^3 -bonded ta-C film (grown using the same method and growth system in this work) changed by $<2\%$ when heated to 650 °C for annealing times up to 4 min. Raman and near-edge x-ray absorption fine structure (NEXAFS) spectroscopies were employed by Anders *et al.*²¹ on ta-C films deposited by cathodic arc and annealed up to 850 °C for 15 min, and they found that while Raman showed only subtle spectral changes, NEXAFS revealed significant increases in the sp^2 character for films annealed above 700 °C. Orwa *et al.* used transmission electron microscopy (TEM) combined with EELS and Raman spectroscopy to determine if the sp^2 bonds ta-C (filtered cathodic arc grown) tend to cluster at higher annealing temperatures (up to 1100 °C). They found that when the films were annealed above 800 °C there was an increase in ordering of graphite-like clusters, and annealing above 1000 °C led to major structural rearrangements and a dramatic increase in the amount of sp^2 bonding.²² Chen *et al.*¹³ conducted fluctuation microscopy studies on ta-C grown by pulsed laser deposition (PLD) using TEM and found, in agreement with Orwa *et al.*, that annealing at 1000 °C induced significant graphitic ordering, and also found that films annealed at lower temperatures (<600 °C) exhibited measurable ordering of sp^3 -bonded carbon without graphitic ordering.

These previous studies have demonstrated how the annealing of ta-C films is accompanied by both rearrangement of the atoms and rehybridization of the bonds, which have important implications regarding the use of ta-C as an engineering material. Here we contribute to this body of work by presenting the use of NEXAFS spectroscopy to quantitatively investigate the changes in the bonding configuration of ta-C as a function of post-deposition annealing temperature. Due to the ability of NEXAFS to detect minute changes in the local carbon bonding hybridization, we are able to confirm that the conversion from sp^3 to sp^2 bonding occurs without passing through an intermediate state, and are able to quantify the activation energy for the conversion of $sp^3 \rightarrow sp^2$ carbon-carbon bonds.

II. EXPERIMENTAL

We prepared ta-C films (130 nm thick) by a PLD process using an excimer laser (Lambda Physik LPX 315i, $\lambda = 248$ nm, 30 ns pulses, 30 Hz repetition rate, 20 min growth time) configured with unstable resonator optics at high fluence (~ 100 J/cm²) to ablate a pyrolytic graphite target in a vacuum chamber ($<1 \times 10^{-6}$ Torr) onto 2.5×10 mm² Si

flats on a rotating holder 12.5 cm from the target. To increase the uniformity, the deposition was performed off-axis such that the laser plume was centered near the edge of the substrate holder. Typically, the deposition thickness within the 5 cm holder diameter varies by less than 5%. All samples were grown in a single deposition run to prevent any systematic variations in film properties. Films grown using the same process were found by ¹³C NMR measurements to contain 80% sp^3 -bonded carbon.¹ We annealed the ta-C films in a rapid thermal annealing oven (Heatpulse 610) under flowing argon at 200 °C intervals up to 1000 °C for 5 min. The samples were ramped to the annealing temperature for 60 s, held for 5 min, and then furnace cooled back to room temperature. The ta-C films annealed at 600 °C exhibited exceptional elastic properties (elastic modulus of ~ 760 GPa and hardness of ~ 80 GPa) (Ref. 3) and superior tribological properties [wear rate of 1×10^{-8} mm³ N⁻¹ m⁻¹, friction coefficient of ~ 0.04 (unpublished values, measured on the stress-relieved ta-C films studied here, to be described in a future publication)].

We performed NEXAFS C 1s measurements on films with and without annealing at beamline 8.0.1 at the Advanced Light Source (ALS) synchrotron in Berkeley, CA. NEXAFS is equally sensitive to sp^3 and sp^2 hybridization states of carbon, and probes the near-surface region of the sample [approximately 4 nm, based on the x-ray penetration depth and the mean free path of electrons in solid carbon (using the known atomic density of ta-C)]. Beamline 8.0.1 is an undulator beam line with energy resolution better than 0.1 eV at ~ 300 eV. The samples were mounted at an angle of 45° with respect to the incident x-ray beam. All measurements were done in total electron yield (TEY) mode. The spectra were first normalized to the absorption current measured simultaneously from a gold mesh placed in the beam line upstream from the measurement chamber, and then normalized based on absorption in the continuum region (315 eV). No subsequent modifications were made to the spectra, which allow for a direct comparison between the samples measured here. We performed Raman measurements with a visible micro-Raman setup using a 10 mW HeNe laser ($\lambda = 632.8$ nm) with a spot size of 1.2 μ m and resolution of ± 1 cm⁻¹. Visible Raman spectroscopy is highly sensitive to sp^2 -hybridized carbon-carbon bonds and has a depth sensitivity on the order of micrometers. For the samples studied here, the entire ta-C films along with a portion of the Si substrate are sampled by the Raman measurements.

III. RESULTS AND DISCUSSION

NEXAFS spectra obtained at the C 1s edge on the as-deposited and annealed ta-C films are shown in Fig. 1(a). For comparison, we obtained a NEXAFS spectrum from a freshly cleaved highly oriented pyrolytic graphite (HOPG) sample, rotated to set the angle between the electric field vector and the c-axis at 54.7° to eliminate polarization dependent effects (dashed line). The C 1s $\rightarrow \pi^*$ peak in the graphite spectrum is located at 285.5 eV, which is the proper location for ordered sp^2 bonding, and the C 1s $\rightarrow \sigma^*$ transition begins at a higher energy (>290 eV) which is a known

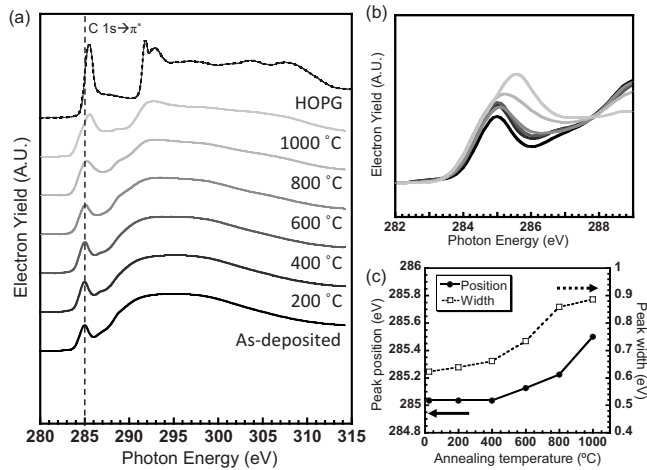


FIG. 1. (a) NEXAFS spectra of an as-deposited ta-C film (black solid line), ta-C films after rapid thermal annealing at various temperatures for 5 min (other solid lines), and a HOPG sample (dashed line). Spectra are normalized in the same manner and offset for clarity. (b) C $1s \rightarrow \pi^*$ peaks for all annealed films plotted on top of one another for comparison. (c) Variations in peak position and peak width of the C $1s \rightarrow \pi^*$ peak as a function of annealing temperature.

characteristic of ordered sp^2 -bonded carbon. The NEXAFS TEY spectrum of as-deposited ta-C exhibits a peak at 285.0 eV due to the C $1s \rightarrow \pi^*$ transition for disordered carbon-carbon sp^2 -hybridized bonds,²¹ and a broad hump starting above 288 eV and extending up to 305 eV due to the C $1s \rightarrow \sigma^*$ transition for disordered carbon-carbon σ bonds. These are all typical features of amorphous carbon films.²³

For the annealed films, there is little change in the spectra until the annealing temperature exceeds 600 °C, above which the C $1s \rightarrow \pi^*$ peak grows in both intensity and width, and shifts to a higher energy. At 800 °C the increase in the C $1s \rightarrow \pi^*$ peak is accompanied by a lowering of the intensity of the broader C $1s \rightarrow \sigma^*$ hump at the lower energies (~ 290 eV). The C $1s \rightarrow \pi^*$ peak in the spectrum from the ta-C film annealed at 1000 °C exhibits a further increase in area and has shifted to a higher energy (~ 285.5 eV). The increase in the integrated area of the C $1s \rightarrow \pi^*$ peak indicates an increase in the sp^2 bonding fraction, the broadening indicates an increase in bond length distribution, and the shift to higher energy indicates an increase in the degree of ordering of the sp^2 bonds. The changes observed for the C $1s \rightarrow \sigma^*$ hump indicate an increase in the average bond length of the σ bonds. The spectrum for 1000 °C has an even greater loss in intensity of the C $1s \rightarrow \sigma^*$ hump around 290 eV than the others. At this annealing temperature, the spectrum begins to substantially resemble the HOPG reference spectrum (dashed line) in Fig. 1.

Figure 1(b) shows the C $1s \rightarrow \pi^*$ peak in greater detail to highlight the trends as a function of annealing temperature, and Fig. 1(c) shows quantitatively how the peak position and peak width increase significantly with increasing annealing temperature above 400 °C. Furthermore, the NEXAFS spectra show that no detectable amount of oxygen or hydrogen is bonded at the surface in either annealed or unannealed ta-C samples, evidenced by the absence of features within the 286–290 eV range. This demonstrates that the flowing argon environment, in which the films were annealed, did not con-

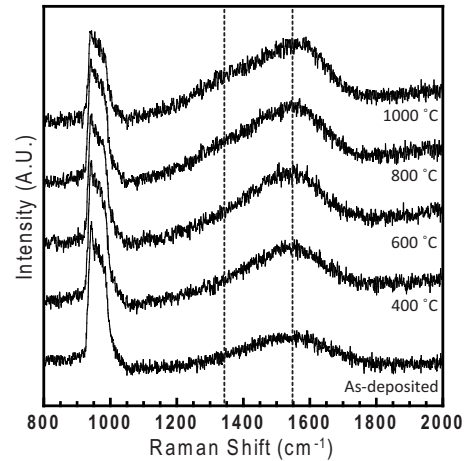


FIG. 2. Raman spectra of as-deposited ta-C film and ta-C films after rapid thermal annealing at various temperatures for 5 min. The dashed lines indicate the positions of the features observed at ~ 1350 and ~ 1550 cm^{-1} . Spectra are offset for clarity.

tain sufficient amounts of either species to react with the surface, thus the surfaces remained purely carbonaceous.

The Raman results for the samples are shown in Fig. 2. At visible laser excitation wavelengths, the Raman signal for threefold carbon is enhanced by $\sim 50\times$ over that from fourfold carbon, thus the broad, symmetric Raman feature near 1550 cm^{-1} is primarily from the threefold bonded carbon (for a review, see Ref. 24). This feature, known in literature as the G peak, is the only feature associated with carbon bonding that is seen for the as-deposited film (the peak at ~ 960 cm^{-1} is from the underlying Si substrate). This G peak is associated with stretching modes of pairs of sp^2 -bonded carbon atoms. As the anneal temperature increases above 400 °C the intensity of the shoulder near 1350 cm^{-1} , known as the D peak, increases, which indicates that sp^2 -bonded carbon sites are organizing into clusters or ringlike structures.^{24,25} This correlates with the changes noted above in the NEXAFS data, whereby spectra from samples annealed at higher temperatures began to exhibit characteristics similar to those of graphite. Additionally, the second order Raman peak for silicon at ~ 960 cm^{-1} decreases with increasing annealing temperature, indicating increased absorption of the ta-C film, presumably from the increased threefold carbon content which has a higher absorption cross section for the Raman process.⁵

The comparison between the NEXAFS spectra and the Raman spectra leads to important conclusions. First, because NEXAFS is a more surface-sensitive technique and Raman samples more of the bulk of the sample, the similar trends observed from both techniques suggest that the ta-C samples are being modified both at the surface and deeper into their bulk. ta-C is expected to have a thin surface layer, approximately 0.5 nm thick,²⁶ that exhibits a stronger sp^2 character compared to the bulk, thus both the surface layer and the underlying bulk contribute to the NEXAFS spectrum (approximately 50% of the NEXAFS signal comes from the top 0.5 nm, as determined by the x-ray penetration depth and the mean free path of electrons in ta-C). Second, because NEXAFS is a more sensitive and linear probe of bonding states,

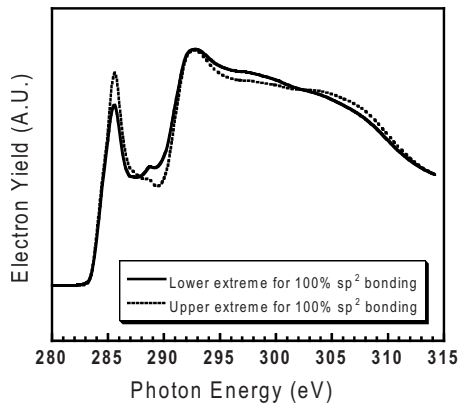


FIG. 3. The two extreme cases for a spectrum representing the 100% sp^2 -bonded amorphous carbon NEXAFS spectrum, extrapolated from the series in Fig. 1 as described in the text. The lower extreme corresponds to the ta-C spectrum annealed at 1000 °C.

analysis of the NEXAFS spectra can produce detailed and quantitative information about the evolution of the hybridization state as a function of temperature.

An isosbestic point at 287.8 eV is observed in the series of NEXAFS spectra [Fig. 1(b)]. This point arose naturally due to the normalization process described in Sec. II, as the data were not shifted or corrected in any other manner. An isosbestic point is a point in a series of absorption spectra where two chemical species have identical absorption coefficients as a reaction proceeds.²⁷ The presence of this isosbestic point is strong evidence that the thermally induced reaction converting sp^3 bonds to sp^2 bonds proceeds without an intermediate step or by forming a by-product, to within the detection limits of NEXAFS. This provides unique evidence to justify the use of a two-state reaction model to describe the thermally driven $sp^3 \rightarrow sp^2$ conversion in ta-C.

Using this observation to validate a two-state model, we were able to approximate a range of activation energies for converting sp^3 - to sp^2 -bonded carbon in ta-C. In this model, each NEXAFS spectrum from the annealed samples in Fig. 1 is recreated by a linear combination of a spectrum from the unannealed ta-C (20% sp^2) and a hypothetical spectrum from a fully converted, 100% sp^2 -bonded spectrum, with the only adjustable parameter being the weighting fraction once the fully converted spectrum is defined. Thus, every spectrum can be uniquely defined by prescribing the weighting fraction using a least-squares fitting routine to maximize the accuracy of the fit to the experimental data. Using these NEXAFS spectra, we extrapolated two extreme cases for this unknown 100% sp^2 -bonded spectrum (Fig. 3). As a “lower” bound, the unknown spectrum would be the 1000 °C spectrum in Fig. 1 (representing full conversion to sp^2 -bonded carbon at 1000 °C); as an “upper” bound, the spectrum would be the most extreme but physically reasonable extrapolated spectrum. We define physically reasonable to mean that the intensity of the NEXAFS spectrum for the fully converted state cannot fall below that of the pre-edge intensity. These upper and lower bounds are then used to define the uncertainty in the sp^2 fraction, quoted using error bars. This procedure yielded the following approximations for sp^2 fractions: 0.39 ± 0.02 , 0.65 ± 0.06 , and 0.91 ± 0.09

for ta-C annealed at 600, 800, and 1000 °C, respectively. We then assumed that the transformation from sp^3 to sp^2 bonding is governed by first order reaction rate theory (as described in Ref. 28). The model described below has been referred to as the Sullivan–Friedmann model and is based on developing an expression for the conversion of sp^3 -bonded carbon to sp^2 bonding as a function of time and temperature. The equation used to calculate the sp^2 fraction as a function of time and temperature is

$$sp^2(t, T) = sp^3(0, 300 \text{ K}) \int_0^\infty N(E_a) [1 - \exp(-\nu_0 t \times \exp(-E_a/k_B T))] dE_a + sp^2(0, 300 \text{ K}), \quad (1)$$

where $sp^3(0, 300 \text{ K})$ is the unannealed sp^3 fraction (0.8), $N(E_a)$ is the distribution of sp^3 fraction versus activation energy (E_a), ν_0 is the attempt frequency typical for solid state reactions [chosen to be 10^{13} s^{-1} (Ref. 28)], k_B is Boltzmann’s constant, and $sp^2(0, 300 \text{ K})$ is the unannealed sp^2 fraction (0.2). $N(E_a)$ was assumed to be a Gaussian distribution normalized to set the area equal to $sp^3(0, 300 \text{ K})$. The mean (x_0) and the standard deviation (σ) were left as free parameters. Equation (1) was evaluated for $t=5$ min with $T=200, 400, 600, 800,$ and 1000 °C, and we fit x_0 and σ using the sp^2 fractions obtained from fits to the experimental data. This analysis yielded a lower-bound activation energy of 3.3 ± 0.7 eV and an upper-bound activation energy of 3.6 ± 0.8 eV. To our knowledge, this is the first attempt at determining an activation energy range for $sp^3 \rightarrow sp^2$ conversion of carbon-carbon bonds in ta-C by analyzing NEXAFS spectra. Ferrari *et al.*²⁹ quantified the changes in the ratio of the intensities of the D and G peaks found in Raman spectra, and they were able to determine an activation energy of ~ 3.3 eV for bulk $sp^3 \rightarrow sp^2$ conversion in ta-C due to post-deposition annealing. Their value is in quantitative agreement with our result (3.5 ± 0.9 eV) and is an encouraging validation of the approach employed here. Furthermore, this agreement affirms that bulk ta-C contributes significantly to the NEXAFS spectra and we are not solely measuring the conversion of a more sp^2 -rich surface layer.

In conclusion, we have shown how changes in the carbon bonding configuration on the surface of ta-C films upon thermal annealing can be probed by NEXAFS. Raman spectroscopy aided in detecting chemical modifications induced by thermal annealing but provided far less detailed information compared to NEXAFS. The presence of an isosbestic point in the NEXAFS spectra provided convincing evidence that sp^2 -hybridized carbon bonds are directly converted to sp^3 -hybridized carbon bonds, thus justifying the use of a two-state model to quantify the activation barrier for rehybridization. We were then able to quantify the significant increases in the amount of sp^2 -bonded carbon in ta-C films heated above 600 °C, and we determined that activation energy for $sp^3 \rightarrow sp^2$ conversion is 3.5 ± 0.9 eV. This is the first time that NEXAFS has been exploited to quantify the energetics of directly converting sp^3 -hybridized carbon bonds into sp^2 -hybridized carbon bonds.

ACKNOWLEDGMENTS

Funding was provided by the Air Force under Grant No. FA9550-08-1-0024. The NEXAFS work was at the ALS which was supported by the DOE under Contract No. DE-AC02-05CH11231. Use of the Center for Nanoscale Materials was supported by the U. S. Department of Energy, Office of Science, Office of Basic Energy Sciences, under Contract No. DE-AC02-06CH11357. The authors would also like to acknowledge help from Dr. J. Denlinger for his assistance with NEXAFS measurements at the ALS.

- ¹K. S. Novoselov, A. K. Geim, S. V. Morozov, D. Jiang, Y. Zhang, S. V. Dubonos, I. V. Grigorieva, and A. A. Firsov, *Science* **306**, 666 (2004).
- ²J. E. Dahl, S. G. Liu, and R. M. K. Carbon, *Science* **299**, 96 (2003).
- ³H. D. Espinosa, B. Peng, N. Moldovan, T. A. Friedmann, X. Xiao, D. C. Mancini, O. Auciello, J. Carlisle, C. A. Zorman, and M. Merhegany, *Appl. Phys. Lett.* **89**, 073111 (2006).
- ⁴A. C. Ferrari, J. Robertson, M. G. Beghi, C. E. Bottani, R. Ferulano, and R. Pastorelli, *Appl. Phys. Lett.* **75**, 1893 (1999).
- ⁵T. A. Friedmann, J. P. Sullivan, J. A. Knapp, D. R. Tallant, D. M. Follstaedt, D. L. Medlin, and P. B. Mirkarimi, *Appl. Phys. Lett.* **71**, 3820 (1997).
- ⁶X. Shi, D. Flynn, B. K. Tay, S. Praver, K. W. Nugent, S. R. P. Silva, Y. Lifshitz, and W. I. Milne, *Philos. Mag. B* **76**, 351 (1997).
- ⁷B. Schultrich, H.-J. Scheibe, D. Drescher, and H. Ziegele, *Surf. Coat. Technol.* **98**, 1097 (1998).
- ⁸G. M. Pharr, D. L. Callahan, S. D. McAdams, T. Y. Tsui, S. Anders, A. Anders, J. W. Ager III, I. G. Brown, C. Singh Bhatia, S. R. P. Silva, and J. Robertson, *Appl. Phys. Lett.* **68**, 779 (1996).
- ⁹S. Anders, A. Anders, I. G. Brown, B. Wei, K. Komvopoulos, J. W. Ager III, and K. M. Yu, *Surf. Coat. Technol.* **68-69**, 388 (1994).
- ¹⁰A. A. Voevodin, A. W. Phelps, J. S. Zabinski, and M. S. Donley, *Diamond Relat. Mater.* **5**, 1264 (1996).
- ¹¹B. Racine, A. C. Ferrari, N. A. Morrison, I. Hutchings, W. I. Milne, and J. Robertson, *J. Appl. Phys.* **90**, 5002 (2001).
- ¹²T. M. Alam, T. A. Friedmann, P. A. Schultz, and D. Sebastiani, *Phys. Rev. B* **67**, 245309 (2003).
- ¹³X. Chen, J. P. Sullivan, T. A. Friedmann, and J. M. Gibson, *Appl. Phys. Lett.* **84**, 2823 (2004).
- ¹⁴A. C. Ferrari, B. Kleinsorge, N. A. Morrison, A. Hart, V. Stolojan, and J. Robertson, *J. Appl. Phys.* **85**, 7191 (1999).
- ¹⁵Y. Lifshitz, G. D. Lempert, and E. Grossman, *Phys. Rev. Lett.* **72**, 2753 (1994).
- ¹⁶X. Shi, L. K. Cheah, J. R. Shi, Z. Sun, and B. K. Tay, *J. Phys.: Condens. Matter* **11**, 185 (1999).
- ¹⁷C. Casiraghi, A. C. Ferrari, R. Ohr, A. J. Flewitt, D. P. Chu, and J. Robertson, *Phys. Rev. Lett.* **91**, 226104 (2003).
- ¹⁸M. Moseler, P. Gumbsch, C. Casiraghi, A. C. Ferrari, and J. Robertson, *Science* **309**, 1545 (2005).
- ¹⁹S. Cho, I. Chasiotis, T. A. Friedmann, and J. P. Sullivan, *J. Micromech. Microeng.* **15**, 728 (2005).
- ²⁰J. M. Jungk, B. L. Boyce, T. E. Buchheit, T. A. Friedmann, D. Yang, and W. W. Gerberich, *Acta Mater.* **54**, 4043 (2006).
- ²¹S. Anders, J. Diaz, J. W. Ager III, R. Y. Lo, and D. B. Bogy, *Appl. Phys. Lett.* **71**, 3367 (1997).
- ²²J. O. Orwa, I. Andrienko, J. L. Peng, S. Praver, Y. B. Zhang, and S. P. Lau, *J. Appl. Phys.* **96**, 6286 (2004).
- ²³G. Comelli, J. Stohr, C. J. Robinson, and W. Jark, *Phys. Rev. B* **38**, 7511 (1988).
- ²⁴A. C. Ferrari and J. Robertson, *Phys. Rev. B* **61**, 14095 (2000).
- ²⁵M. Chhowalla, A. C. Ferrari, J. Robertson, and G. A. J. Amaratunga, *Appl. Phys. Lett.* **76**, 1419 (2000).
- ²⁶C. Casiraghi, A. C. Ferrari, R. Ohr, D. Chu, and J. Robertson, *Diamond Relat. Mater.* **13**, 1416 (2004).
- ²⁷A. D. McNaught and A. Wilkinson, *IUPAC Compendium of Chemical Terminology*, 2nd edition (Blackwell Science, Oxford, 1997).
- ²⁸J. P. Sullivan, T. A. Friedmann, and A. G. Baca, *J. Electron. Mater.* **26**, 1021 (1997).
- ²⁹A. C. Ferrari, S. E. Rodil, J. Robertson, and W. I. Milne, *Diamond Relat. Mater.* **11**, 994 (2002).